DOI: 10.1002/ejic.200500960

Novel Coordination Polymers Generated from Angular 2,2′-Dipyridyl Ligands and Bis(hexafluoroacetylacetonate) Copper(II): Crystal Structures and Magnetic Properties

Salomé Delgado,*[a] Aitor Barrilero,[a] Agustín Molina-Ontoria,[a] Manuela E. Medina,[b] Cesar J. Pastor,[b] Reyes Jiménez-Aparicio,[c] and José L. Priego[c]

Keywords: Coordination polymers / Copper / N ligands

The synthesis of the ligand 2,5-bis(2-pyridylethynyl)thiophene (**L2**) is described and the coordination chemistry of the 2,2′-long conjugated bidentate ligands 1,2-di(2-pyridyl)-butadiyne (**L1**), 2,5-bis(2-pyridylethynyl)thiophene (**L2**), and 2,2′-dipyridyl disulfide (**L3**) with $Cu(hfac)_2$ (hfac = hexafluoroacetylacetonate) is investigated. Three new coordination polymers $\{[Cu(hfac)_2L]_n$ (**1** for L = **L1**, **2** for L = **L2** and **3** for L = **L3**)} are prepared and fully characterized by infrared spectroscopy, elemental analysis, thermogravimetric analysis, and X-ray diffraction. They are obtained by a combination of **L1**, **L2**, or **L3** with $Cu(hfac)_2{\cdot}H_2O$ in dichloromethane (CH_2Cl_2) as the solvent. When CH_2Cl_2 solutions of **3** were left standing for longer than one day or were refluxed for two days, rearrangements took place and **3** was transformed into **4** and **5**. Compounds **1**–**3** adopt a one-dimensional chain structure with the copper atom in a six-coordinate 4+2 pseudooctahedral geometry. In **1** and **2**, four equatorial sites Cu–O/N and two axial sites Cu–O are found with an unusual *cis* orientation of two $\mathbf{L_1}$ or $\mathbf{L_2}$ ligands, respectively, while in **3** the four equatorial sites are defined by four oxygen atoms from two hfac chelating ligands and the axial sites by two nitrogen donors from two *trans*-**L3** ligands. Compound **4** contains a (1-hydro-2-pyridinio)thio group that is bound to a hexafluoroacetylacetonate anion through a S–C bond and **5** is a molecular compound where the Cu^{II} ion is pentacoordinate to two oxygen atoms of the hfac anion, two nitrogen atoms of two 2-pyridyl sulfide fragments, and one carbon atom of the $CC(O)CF_3$ fragment, which has been inserted into the S–S bond of the 2,2′-dipyridyl disulfide ligand, giving a new tridentate ligand. The reaction of **L3** with copper acetate leads to the molecular 1:2 adduct $Cu_2(\mu\text{-}OAc)_4(L3)_2$ (**6**), where the Cu^{II} ion is pentacoordinate to four oxygen atoms of four different acetate anions and one nitrogen atom from the pyridine ring of **L3** to form a square-pyramidal geometry.

Introduction

The rational design of new coordination polymers is of current interest in the field of supramolecular chemistry and crystal engineering because of their exploitable properties; these include magnetism,[1] catalysis and separation,[2] non-linear optics,[3] and molecular sensing.[4] Coordination polymers with diverse architectures, such as linear or zigzag chains, helices, honey-combs, square grids, ladders, brick walls, and interwoven diamondoids have been extensively developed.[5] In particular, much research has been concentrated on the use of bridging 4,4′-bipyridyne-based rodlike ligands,[6] whereas bent ligands are relatively less frequently used as building blocks because of the difficulty in predicting the structure. Recently, crystalline polymers have been synthesized by using 1,2-di(3-pyridyl)ethyne or 2,5-di(3-pyridyl)-1,3,4-oxadiazole and Cd^{II}, Co^{II}, Cu^{II} salts.[7] Moreover, unsaturated metal complexes such as bis(hexafluoroacetylacetonate)metal(II) are promising metal building blocks and have proved to be very useful precursors in the synthesis of several types of molecular materials including thin metallic and oxide films and magnetic materials.[8–10]

With this in mind, the aim of this work is to study the effect of the 2,2′-positional orientation of the nitrogen atoms in *N*,*N*′-bidentate ligands on the coordination framework and to affect the polymeric architectures of the crystalline materials. Ligands with nitrogen atoms at the 2-position of the pyridyl ring do not readily form polymeric compounds, as is the case for ligands with nitrogen atoms at the 3- and 4-positions. Therefore, the reaction between 1,2-di(2-

[a] Departamento de Química Inorgánica de la Universidad Autónoma de Madrid,
28049 Madrid, Spain
E-mail: salome.delgado@uam.es
[b] Servicio Interdepartamental de Investigación, Laboratory of Single Crystal X-ray Diffraction, Universidad Autónoma de Madrid,
28049 Madrid, Spain
[c] Departamento de Química Inorgánica. Facultad de Ciencias Químicas, Universidad Complutense de Madrid, Ciudad Universitaria,
28040 Madrid, Spain

pyridyl)ethyne and $Cu(hfac)_2$ only formed solutions when a methanol solution of ligand was layered over a dichloromethane solution of copper(II) hexafluoroacetylacetonate.[11]

In this report, we focus on 1,2-di(2-pyridyl)butadiyne (**L1**), 1,2-bis(2-pyridylethynyl)thiophene (**L2**), and 2,2′-dipyridyl disulfide (**L3**), in which the first two are rigid ligands and the last one is a flexible ligand that may assume a twisted conformation because of the flexible –S–S– bridging group. The C–S–S–C torsion angles in aromatic disulfides are known to be generally within a range of 70–90°.[12a] Further, oxidation of 2,2′-dipyridyl disulfide to pyridine-2-sulfinate in the presence of the Cu^{II} ion and water has been reported.[12b] Here we describe the synthesis, structures, and properties of new Cu^{II} coordination polymers. The 1,2-bis(2-pyridylethynyl)thiophene ligand was synthesised and used first as a linker.

Results and Discussion

When dichloromethane solutions of **L1** and **L2** were allowed to diffuse, at room temperature, into a solution of $Cu(hfac)_2$ in the same solvent (ratio 1:1), the infinite coordination polymers **1** and **2** were afforded as green and yellow crystalline materials, respectively, within 2–3 days. Similar results were obtained when layering the dichloromethane solution of copper(II) hexafluoroacetylacetonate over a solution of **L1** or **L2**.

Treatment of $Cu(hfac)_2$ with 2,2′-dipyridyl disulfide (**L3**), depending on the conditions, leads to the formation of different products. When a methanol solution of **L3** is allowed to diffuse, at room temperature, into a solution of $Cu(hfac)_2$ in the same solvent, the coordination polymer **3** is obtained as a green solid after one day. By contrast, when the reaction is carried out in CH_2Cl_2, under similar conditions, **3** is also isolated together with the orange organic compound **4** and the violet mononuclear compound **5** as minor products. The amount of **3** diminished significantly and the yield of **4** and **5** increased up to 50% after prolonged standing in contact with CH_2Cl_2. If the same reagents are allowed to react together under reflux in CH_2Cl_2 or MeOH for two days, only **4**, as the major product, and **5** are obtained. During this process **3** is converted into 2-[(1-hydro-2-pyridinio)thio]hexafluoroacetylacetonate (**4**) and the mononuclear compound **5**, where a new copper–carbon bond is formed (Scheme 1). Crystals of **3** can be stored unchanged at room temperature. It is also stable in ether or CCl_4 solutions but slowly decomposes to **4** and **5** in acetone solutions. In order to explain the formation of complexes **4** and **5** from **3**, we have carried out additional experiments. In order to test whether H_2O or O_2 play a role in the formation of the final products, we have repeated the

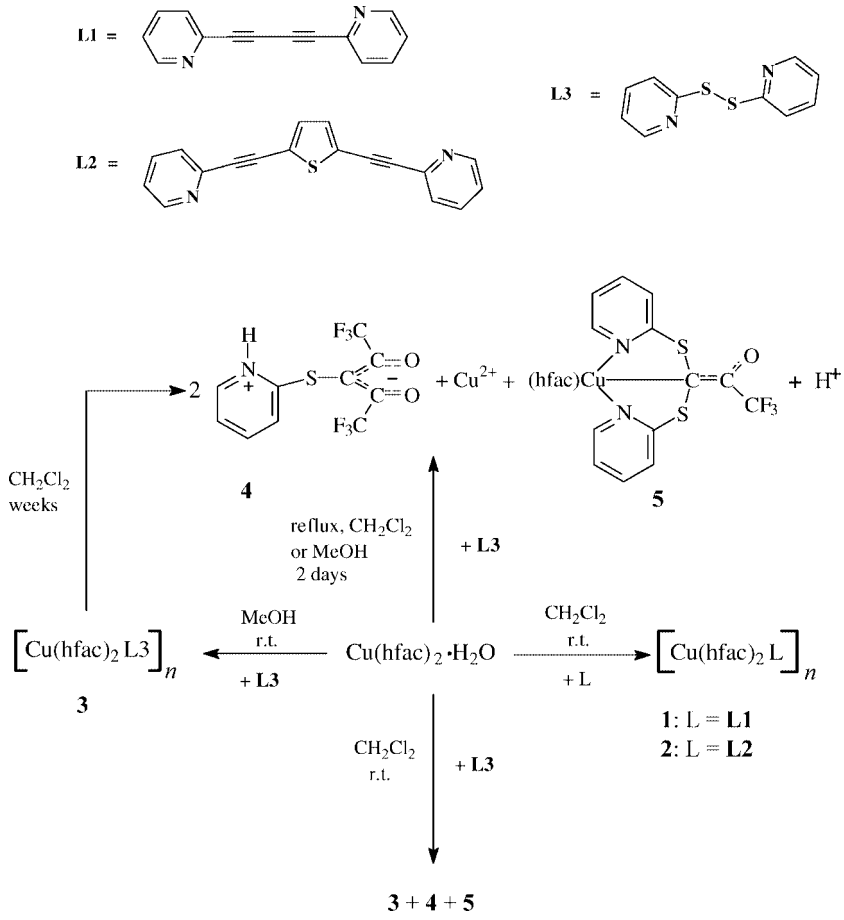

Scheme 1.

reactions, in CH_2Cl_2 at reflux, under both anaerobic and anhydrous conditions, and monitored the reactions by FT-IR spectroscopy until the strong $\nu_{C\equiv O}$ band at 1641 cm^{-1} assigned to **3** disappeared. However, the results were similar to those previously obtained.

One possible mechanism that could explain the formation of **4** and **5** from **3** involves the homolytic cleavage of the S–S bond in the **L3** ligand, probably promoted by the Cu^{II} ion. It is known that the disulfide bond in R–S–S–R–systems is broken by metal ions.[12b] The attack of the imine carbon atom of the $hfac^-$ anion on the sulfur atom of the pyridyl sulfide radical leads to the formation of **4**. This pathway is predominant because **4** is obtained in higher yield than **5**. Along with this, some $hfac^-$ is broken apart and $C(H)C(O)CF_3$ fragments are bonded to the sulfur atom of pyridyl sulfide to give **5**, probably via the formation of an intermediate with an acid proton, which is easily removed by the stabilization that allows the formation of two five-membered rings. The CF_3–C(O) fragments could be recombined to produce the 1,2-diketone F_3C–C(O)–C(O)–CF_3, which could not be detected because of its high volatility (b.p. = 19 °C). Some of the CF_3–C(O) fragments could also lead to CHF_3 and CO, but neither of these were detected during the reaction (Scheme 2).

Finally, when $Cu(OAc)_2{\cdot}H_2O$ dissolved in methanol is reacted at room temperature with **L3** in methanol in a 1:1 molar ratio, a green solution is obtained. After workup, green crystals of the molecular 1:2 adduct $Cu_2(\mu\text{-}OAc)_4(L3)_2$ (**6**) were obtained. The polymeric compound was not formed. This complex dissociates to $Cu(OAc)_2{\cdot}H_2O$ and **L3** after prolonged standing in contact with the solution.

All compounds have been characterized by analytical and IR spectroscopic data. Details are given in the Experimental Section. In the IR spectra of **1** and **2**, the ν(CO) stretching bands appear to be split into two bands (1654, 1592 $cm^{-1}$and 1644, 1594 cm^{-1}, respectively) while in **3** only one ν(CO) is observed (1641 cm^{-1}). This is consistent with a pseudooctahedral geometry around the copper(II) ion (see the description of the structures). In **1** and **2** the former bands are assigned to the stretching of C(4)=O(3),

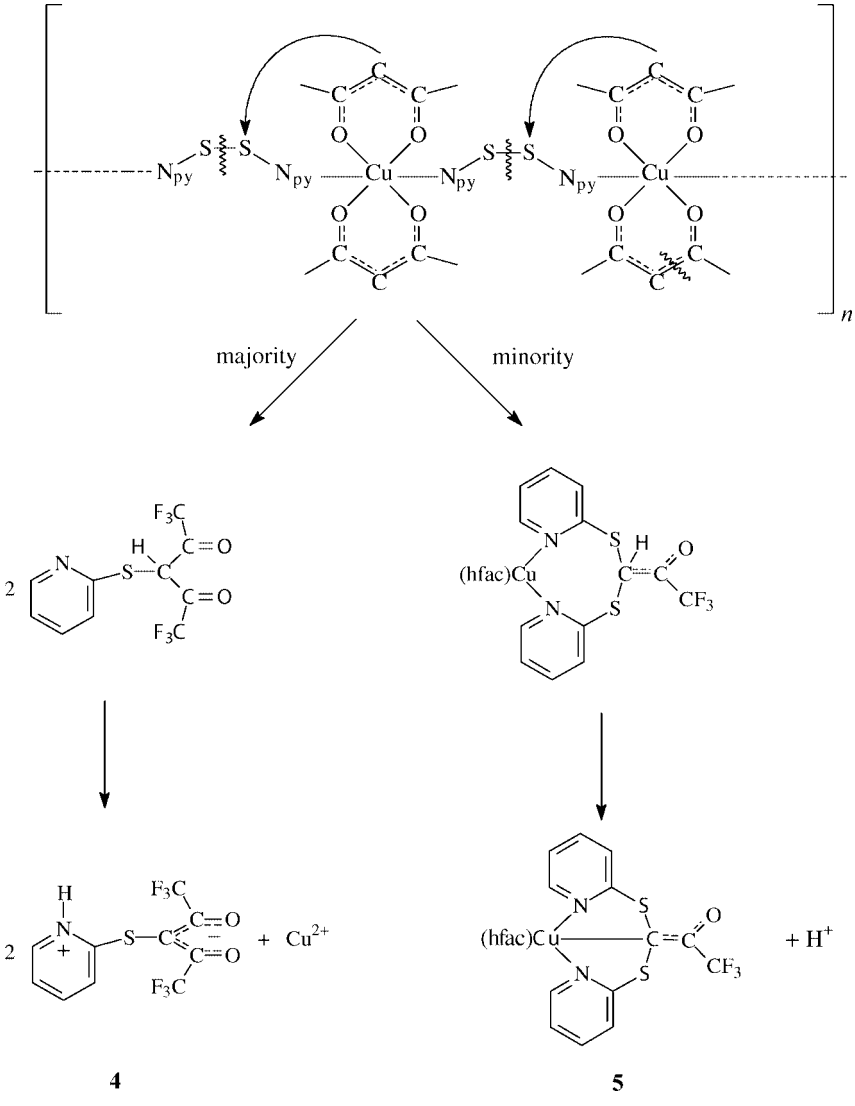

Scheme 2.

C(24)=O(3) and C(3)=O(2), C(21)=O(2), respectively; these oxygen atoms are more strongly bonded to the Cu^{II} ion, and the latter to C(1)=O(1), C(19)=O(1) and C(6)=O(4), respectively. In **3**, the four (C=O) distances of the two hfac rings have similar values. In the IR spectrum of **4** a single ν(CO) band is observed at 1679 cm^{-1}, at a higher energy than those for polymers **1**–**3**, which is in accordance with the shorter (C–O) bond. Moreover, a ν(N–H) band is located at 3103 cm^{-1}, and a ν(C=N) band and three ν(C=C) bands at 1606, 1583, 1452, and 1420 cm^{-1}, respectively, are observed. The latter four bands are shifted to a higher energy with respect to the free ligand (1570, 1556, 1443, and 1416 cm^{-1}, respectively); the same behavior is observed when pyridine and pyridinium ligands are compared. Finally, at 838 cm^{-1} a new band appears that can be attributed to a (C–S) vibration of the new bond, which has formed. In the IR spectrum of **5**, two types of ν(CO) stretching bands are observed. A single (CO) band at 1673 cm^{-1}, attributed to the stretching of C(30)=O(6) from the –C–C(O)–CF_3 fragment and a (CO) stretching band with two peaks at 1650 and 1611 cm^{-1} from the chelating hfac ligand. As in **1** and **2**, the first band is assigned to the stretching of C(32)=O(4), which is more strongly bonded to the Cu^{II} ion, and the second to C(34)=O(5).

For **6** the characteristic bands of the acetate anions appear at 1620 ν_{as}(C–O), 1427 ν_{sym}(C–O) and 682 δ(O–C–O) cm^{-1} together with the absorption bands resulting from the aromatic rings in the 1400–1600 cm^{-1} range. The Δ value ($\nu_{as} - \nu_{sym}$) indicates that the acetate anion coordinates to the Cu^{II} center in a bridging mode.

Description of the Crystal Structures

[Cu(hfac)$_2$L1]$_n$ (1)

The crystallographic data are given in Table 1 (compounds **1**–**3**). An ORTEP view of a copper center is shown in Figure 1 (a), together with the atom numbering scheme. Selected bond lengths and angles are listed in Table 2. The coordination geometry of the copper(II) ion is pseudooctahedral in which four oxygen atoms from two hfac ligands chelate to the Cu^{II} center, while the other two sites are occupied by two nitrogen atoms from two *cis*-1,2-di(2-pyridyl)-butadiyne ligands. The pyridyl groups of the **L1** ligand are coplanar through the diyne portion. Usually a *trans* orientation of the pyridine rings is adopted in these types of complexes [Cu(hfac)$_2$L$_2$] [L = pyrazine,[13] 1,2-di(2-pyridyl)-ethyne][7] or the analogous 1,2-bis(3-pyridyl)butadiyne ligand.[14] This different behavior suggests that the relative orientation of the pyridyl nitrogen donors can control the coordination framework and influence the polymeric architectures of the crystalline materials. To the best of our knowledge, a *cis* orientation has only been found in [Cu(hfac)$_2$(4-PDS)] (4-PDS = 4,4′-dipyridyl disulfide).[15] As already known, Cu^{II} is Jahn–Teller-active, so it is expected to adopt a 4+2 coordination environment with two long bond lengths and four shorter ones, as is usually observed. As a result of this, the bond angles within the CuO_4N_2 octahedra deviate appreciably from 90° and vary from 81.61(5) to 100.57(6)° for O(2)–Cu(1)–O(1) and N(2)–Cu(1)–O(4), respectively. Similar types of distorted coordination geometries are reported for [Cu(hfac)$_2$L]$_n$ complexes.[16,17] In addition to this, the N(2)–Cu(1)–N(1) bond angle, which is 96.37(6)°, deviates from a perfect right angle.

The Cu–N bond length of 2.0438(2) Å in **1** is intermediate between the Cu–N bond length found in the Cu(hfac)$_2$ complexes with 1,2-bis(3-pyridyl)ethyne {2.061(3) Å}[7] and 1,2-bis(3-pyridyl)butadiyne {2.026(2) Å};[15] and significantly longer than that in the polymeric compound [Cu(hfac)$_2${1,2-bis(4-pyridyl)ethane}]$_n$ [Cu–N 2.014 (7) Å].[13]

Two copper centers bond through the N1 and N2 atoms of two $\mathbf{L_1}$ molecules in a *transoid* conformation forming dimers. As a result of this, the extended structure consists of polymeric 1D chains that run parallel to the *b* axis as is shown in Figure 2, where the **L1** ligand links the Cu(hfac)$_2$ moieties together. The intra- and interpolymer Cu···Cu distances are 8.950 Å and 8.221 Å, respectively. Because **L1** affords close contact between neighboring polymeric chains, the interpolymeric Cu···Cu distance is significantly shorter than that in the polymer constructed from the 1,2-bis(3-pyridyl)butadiyne ligand (13.88 Å).[14] Surprisingly, no interpolymer hydrogen-bonding interactions were found.

[Cu(hfac)$_2$L2]$_n$ (2)

The crystallographic data are given in Table 1 (compounds **1**–**3**). Selected bond lengths and angles are listed in Table 3. The structure, emphasizing the coordination environment around the copper atom, is shown in Figure 1 (b). As in **1**, the copper atom has a six-coordinate 4+2 pseudo-octahedral geometry defined by two nitrogen donors from two *cis*-**L2** ligands and four oxygen donors from two hfac chelating ligands. In contrast, the pyridyl groups of the **L2** ligand are not coplanar through the diyne portion and form an angle of 68°. The Cu–N and Cu–O bond lengths are very close to those found in compound **1**. In contrast to **1**, the two Cu(hfac)$_2$ units of compound **2** are joined by the **L2** ligand in a *cisoid* conformation. The structure of **2** consists of one-dimensional chains running parallel to the *a* axis, as is shown in Figure 3. The intra- and interpolymer Cu···Cu distances are 9.421 Å and 10.983 Å, respectively. Interpolymer hydrogen bonding was not observed.

[Cu(hfac)$_2$L3]$_n$ (3)

An ORTEP view of the copper center is shown in Figure 4 (a), together with the atom numbering scheme. Table 1 (compounds **1**–**3**) gives the crystallographic data for **3**, while selected bond lengths and angles are listed in Table 4. In this compound the copper atom has a six-coordinate 4+2 pseudooctahedral geometry, where the four equatorial sites are defined by four oxygen atoms from two hfac chelating ligands (1.9365 Å to 1.9572 Å), but in contrast to compounds **1** and **2**, the axial sites have two nitrogen donors from two *trans*-**L3** ligands. This is unusual because four equatorial sites Cu–O/N and two axial sites Cu–O are

Table 1. Crystallographic data for compounds **1** to **3** and compounds **4** to **6**.

	1	**2**	**3**
Empirical formula	$C_{24}H_{10}CuF_{12}N_2O_4$	$C_{28}H_{12}CuF_{12}N_2O_4S$	$C_{20}H_{10}CuF_{12}N_2O_4S_2$
Molecular mass [g/mol]	681.88	764.00	697.96
Temperature [K]	100(2)	100(2)	100(2)
Wavelength [Å]	1.54178	1.54178	1.54178
Crystal system	monoclinic	tricilinic	monoclinic
Space group	*P*21/*n*	$P\bar{1}$	*P*21/*n*
Unit cell dimensions	*a* = 13.0798(1)	*a* = 9.4206(1)	*a* = 17.2605(8)
a, *b*, *c* [Å]	*b* = 15.6050(1)	*b* = 10.4051(1)	*b* = 8.1387(7)
α, *β*, *γ* [°]	*c* = 13.3245(1)	*c* = 15.5323(1)	*c* = 19.1467(1)
	α = 90	*α* = 81.8410(1)	*γ* = 90
	β = 107.465(1)	*β* = 75.1390(1)	*β* = 115.396(3)
	α = 90	*γ* = 80.9270(10)	*γ* = 90
Volume [Å^3]	2594.29(3)	1444.94(2)	2429.8(3)
Z	4	2	4
Density (calculated) [mg/m^3]	1.746	1.756	1.908
Absorption coefficient [mm^{-1}]	2.339	2.838	4.075
F(000)	1348	758	1380
Crystal size [mm]	0.25 × 0.20 × 0.12	0.20 × 0.20 × 0.10	0.20 × 0.18 × 0.06
Theta range for data collection [°]	4.15 to 70.62	2.96 to 70.52	2.89 to 69.15
Index ranges	$-15 \le h \le 15$	$-11 \le h \le 10$	$-20 \le h \le 20$
	$-18 \le k \le 19$	$-12 \le k \le 12$	$-9 \le k \le 9$
	$-15 \le l \le 16$	$-18 \le l \le 18$	$-23 \le l \le 22$
Reflections collected	16356	14930	18573
Independent reflections	4769	5225	4378
	[*R*(int) = 0.0258]	[*R*(int) = 0.0260]	[*R*(int) = 0.0477]
Completeness to *θ* = 70.62°/70.52°/69.15° [%]	95.9	94.2	96.6
Absorption correction		semi-empirical from equivalents	
Refinement method		full-matrix least-squares on F^2	
Data/restraints/parameters	4769/0/428	5225/0/535	4378/0/413
Goodness-of-fit on F_2	1.048	1.037	1.023
Final *R* indices [$I > 2\sigma(I)$]	R_1 = 0.0337	R_1 = 0.0346	R_1 = 0.0324
	wR_2 = 0.0878	wR_2 = 0.0903	wR_2 = 0.0819
R indices (all data)	R_1 = 0.0361	R_1 = 0.0381	R_1 = 0.0416
	wR_2 = 0.0894	wR_2 = 0.0927	wR_2 = 0.0876
Largest diff. peak and hole [e/Å^3]	0.758 and –0.498	0.485 and –0.369	0.426 and –0.482
	4	**5**	**6**
Empirical formula	$C_{10}H_5F_6NO_2S$	$C_{18}H_9CuF_9N_2O_3S_2$	$C_{28}H_{28}Cu_2N_4O_8S_4$
Molecular mass [g/mol]	317.21	599.93	803.86
Temperature [K]	100(2)	100(2)	100(2)
Wavelength [Å]	1.54178	1.54178	1.54178
Crystal system	monoclinic	monoclinic	monoclinic
Space group	*C*2/*c*	*P*21/*c*	*P*21/*c*
Unit cell dimensions	*a* = 17.4388(4)	*a* = 17.3908(3)	*a* = 7.9211(9)
a, *b*, *c* [Å]	*b* = 11.0843(2)	*b* = 15.5348(2)	*b* = 26.961(3)
α, *β*, *γ* [°]	*c* = 13.8206(4)	*c* = 17.2529(2)	*c* = 7.6840(10)
	α = 90	*α* = 90	*α* = 90
	β = 117.039(2)	*β* = 116.1050(1)	*β* = 93.393(4)
	γ = 90	*γ* = 90	*γ* = 90
Volume [Å^3]	2379.48(1)	4185.60(1)	1638.1(3)
Z	8	8	2
Density (calculated) [mg/m^3]	1.771	1.904	1.630
Absorption coefficient [mm^{-1}]	3.241	4.353	4.454
F(000)	1264	2376	820
Crystal size [mm]	0.20 × 0.08 × 0.03	0.20 × 0.18 × 0.09	0.16 × 0.10 × 0.08
Theta range for data collection[°]	4.90 to 69.27	2.83 to 68.27	3.28 to 68.74
Index ranges	$-21 \le h \le 19$	$-20 \le h \le 20$	$-9 \le h \le 8$
	$-13 \le k \le 13$	$-18 \le k \le 18$	$-28 \le k \le 32$
	$-14 \le l \le 16$	$-20 \le l \le 20$	$-8 \le l \le 9$
Reflections collected	9377	31380	9381
Independent reflections	2175	7549	2932
	[*R*(int) = 0.0275]	[*R*(int) = 0.0370]	[*R*(int) = 0.0589]
Completeness to *θ* = 69.27°/68.27°/68.74° [%]	97.3	98.6	96.8
Absorption correction		semi-empirical from equivalents	
Refinement method		full-matrix least-squares on F^2	
Data/restraints/parameters	2175/0/201	7549/0/631	2932/0/210
Goodness-of-fit on F^2	1.033	1.035	1.036
Final *R* indices [$I > 2\sigma(I)$]	R_1 = 0.0277	R_1 = 0.0317	R_1 = 0.0457
	wR_2 = 0.0736	wR_2 = 0.0777	wR_2 = 0.1116
R indices (all data)	R_1 = 0.0305	R_1 = 0.0373	R_1 = 0.0597
	wR_2 = 0.0760	wR_2 = 0.0812	wR_2 = 0.1213
Largest diff. peak and hole [e/Å^3]	0.338 and –0.233	0.523 and –0.360	0.900 and –0.386

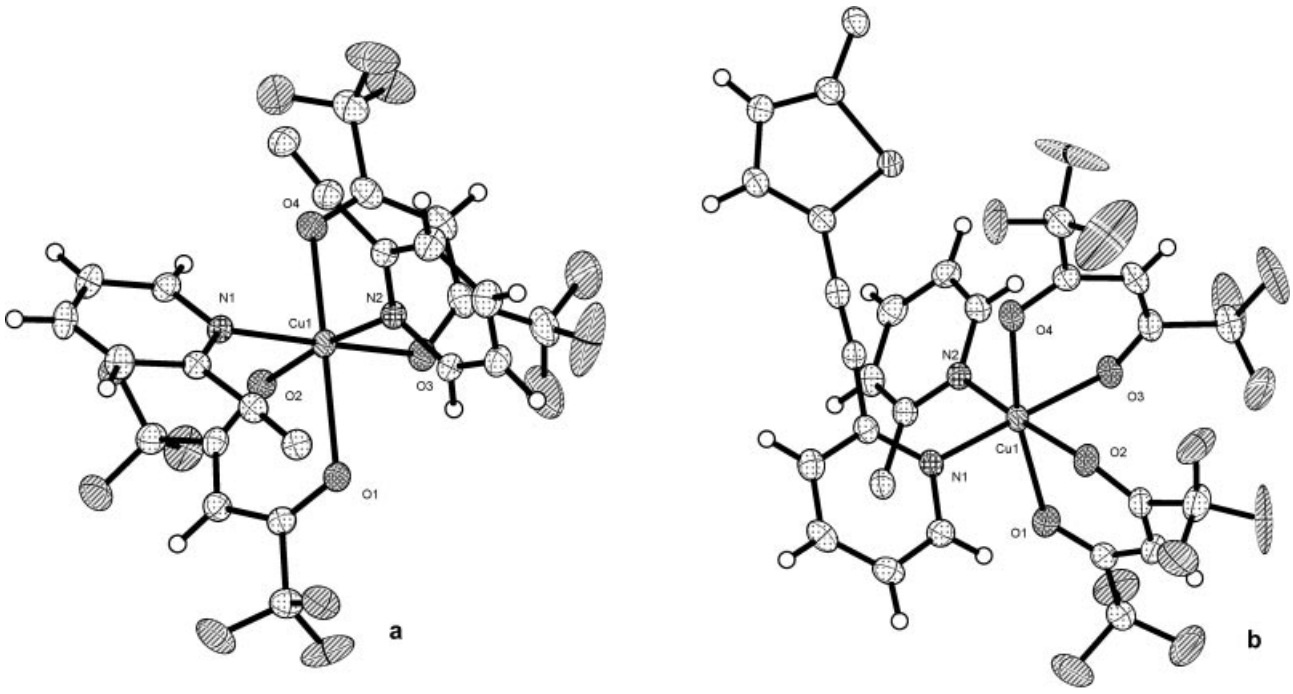

Figure 1. **a**: Molecular structure of **1**, **b**: molecular structure of **2** (displacement ellipsoids are shown at the 50% probability level).

Table 2. Selected bond lengths and angles for compound **1**.

Selected bond lengths [Å]	Selected angles [°]	
Cu(1)–O(3) 1.9927(1)	O(3)–Cu(1)–O(2) 89.84(6)	N(2)–Cu(1)–O(4) 100.57(6)
Cu(1)–O(2) 2.0133(1)	O(3)–Cu(1)–N(2) 87.31(6)	N(1)–Cu(1)–O(4) 90.97(6)
Cu(1)–N(2) 2.0348(2)	O(2)–Cu(1)–N(2) 173.28(6)	O(3)–Cu(1)–O(1) 85.92(5)
Cu(1)–N(1) 2.0438(2)	O(3)–Cu(1)–N(1) 175.51(6)	O(2)–Cu(1)–O(1) 81.61(5)
Cu(1)–O(4) 2.2408(1)	O(2)–Cu(1)–N(1) 86.77(6)	N(2)–Cu(1)–O(1) 92.12(6)
Cu(1)–O(1) 2.3225(1)	N(2)–Cu(1)–N(1) 96.37(6)	N(1)–Cu(1)–O(1) 96.48(6)
C(3)–O(2) 1.2690(2)	O(3)–Cu(1)–O(4) 85.82(6)	O(4)–Cu(1)–O(1) 164.50(5)
C(4)–O(3) 1.259(3)	O(2)–Cu(1)–O(4) 85.28(5)	
C(6)–O(4) 1.232(3)		

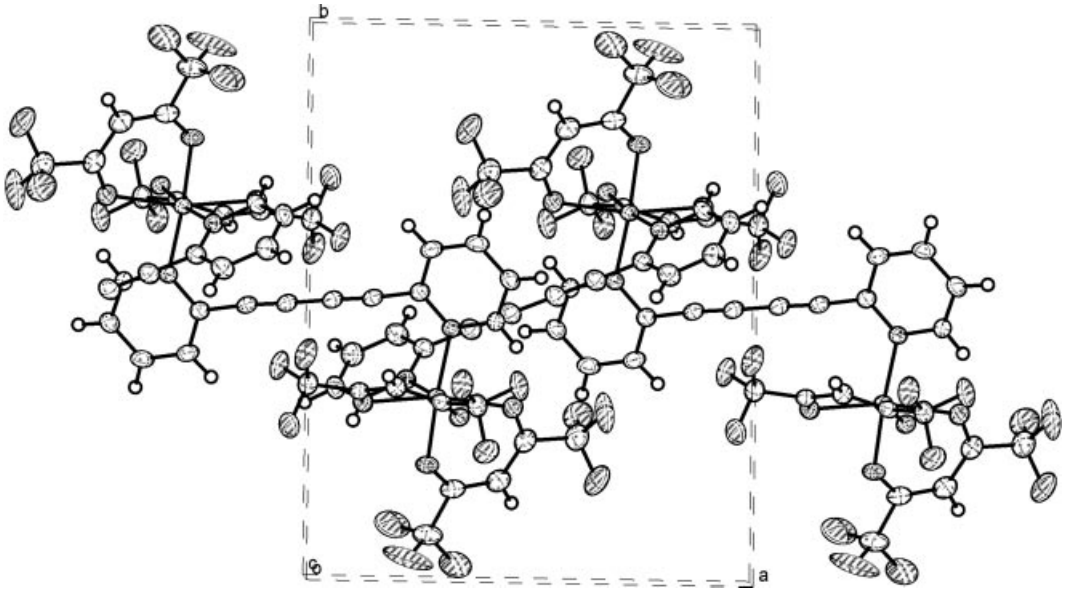

Figure 2. View of the one-dimensional chain formed by compound **1**. The chains are shown along the crystallographic *a* axis.

Table 3. Selected bond lengths and angles for compound **2**.

Selected bond lengths [Å]	Selected angles [°]	
Cu(1)–O(2) 2.0145(15)	O(2)–Cu(1)–O(3) 84.09(6)	N(1)–Cu(1)–O(4) 90.09(6)
Cu(1)–O(3) 2.0155(15)	O(2)–Cu(1)–N(1) 88.85(6)	N(2)–Cu(1)–O(4) 96.82(6)
Cu(1)–N(1) 2.0379(16)	O(3)–Cu(1)–N(1) 171.74(6)	O(2)–Cu(1)–O(1) 84.58(6)
Cu(1)–N(2) 2.0408(17)	O(2)–Cu(1)–N(2) 172.29(6)	O(3)–Cu(1)–O(1) 87.33(6)
Cu(1)–O(4) 2.2739(15)	O(3)–Cu(1)–N(2) 89.29(6)	N(1)–Cu(1)–O(1) 96.29(6)
Cu(1)–O(1) 2.2750(15)	N(1)–Cu(1)–N(2) 98.03(6)	N(2)–Cu(1)–O(1) 91.19(6)
	O(2)–Cu(1)–O(4) 86.58(6)	O(4)–Cu(1)–O(1) 168.98(5)
	O(3)–Cu(1)–O(4) 85.22(6)	

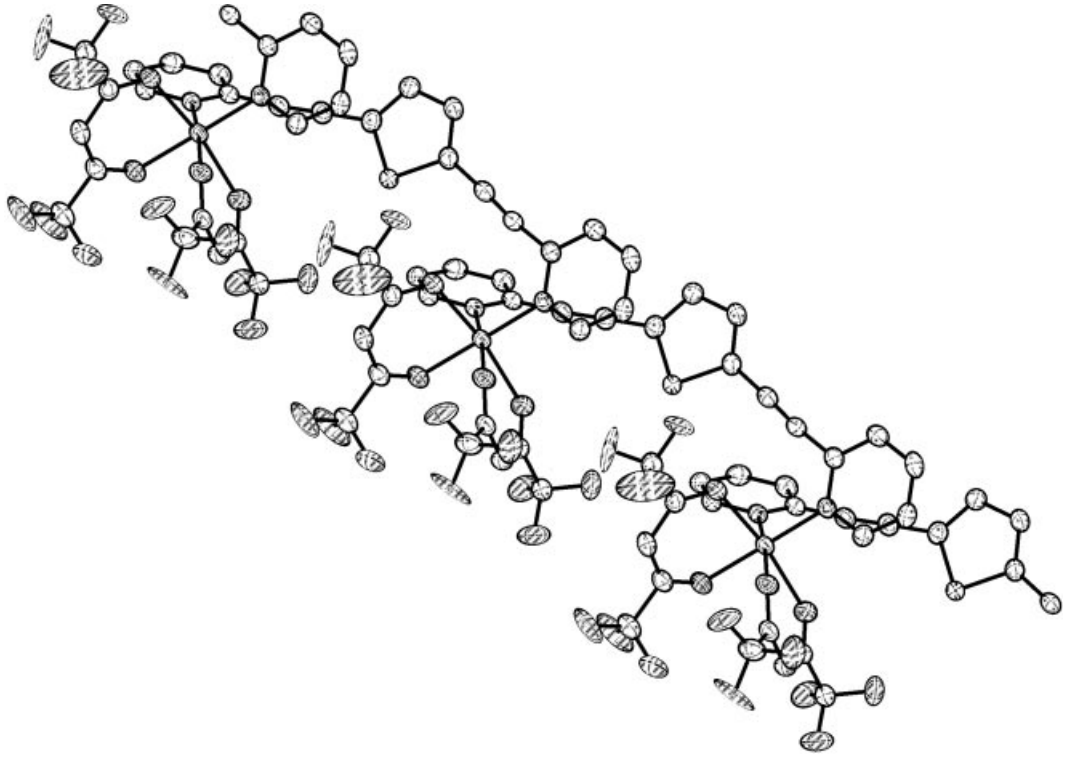

Figure 3. View of the one-dimensional chain architecture of **2**. The chains are shown along the crystallographic *a* axis.

found in $L_2Cu(hfac)_2$ type complexes. The Cu–N bond lengths are 2.4587(19) and 2.5968(19) Å, unexpectedly longer than distances found in copper dipyridyl disulfide compounds[14,15,18] or in N-donor-coordinated $Cu(hfac)_2$ complexes, including **1** and **2**. A similar distance is reported for $[Cu(hfac)_2(pyz)]$ [2.529(9) Å][19a] and $Cu(hfac)_2$(ted) [2.566(7) Å].[19b] One possible explanation for these very long Cu–N bonds is the interaction of the pyridine rings with the hfac ring (see part a in Figure 4). The intramolecular geometry of the **L3** ligand shows a C–S–S–C torsion angle of 79.8(10)°, smaller than that in the free ligand (87.1°) and in the analogous $Cu(hfac)_2$(4,4′-dipyridyl disulfide)[15] [88.1(2)°], which seems to indicate a slight deformation when **L3** is coordinated to the metal ion. The S–S bond length of 2.0369(8) Å is in close agreement with the value found in the free **L3** ligand [2.016(2)].[20] The angle between the two pyridyl rings is 79.83(10)°. Compound **3** assumes a one-monodimensional zigzag chain structure, as shown in part b of Figure 4, where each copper center is bridged by the twisted ligands of 2,2′-dipyridyl disulfide in a *cisoid* conformation. The interchain and intrachain Cu–Cu distances are 8.139 and 9.573 Å, respectively.

2-[(1-Hydro-2-pyridinio)thio]hexafluoroacetylacetonate (4)

The structure is shown in Figure 5 (a) together with the atom numbering scheme. Crystallographic data are given in Table 1 (compounds **4**–**6**), and the selected bond lengths and angles are listed in Table 5. The molecule adopts a nonplanar disposition. The pyridinium ring is oriented almost perpendicular to the hexafluoroacetylacetonate anion (89.75°). The intramolecular geometry of the hexafluoroacetylacetonate anion shows O–C–C, C–C–C, and C–S–C torsion angles of 126.40(13), 118.66(12), and 104.84(7)°, respectively; these values are comparable to those found for compound **3** [128.2(2), 121.1(2), and 104.64(8)°, respectively] and indicates that the $hfac^-$ moiety seems to maintain its characteristic shape. The C–S distances are 1.7573(15) and 1.7601(14) Å, which are similar to those found in other copper dipyridyl disulfide compounds[15,18] and slightly

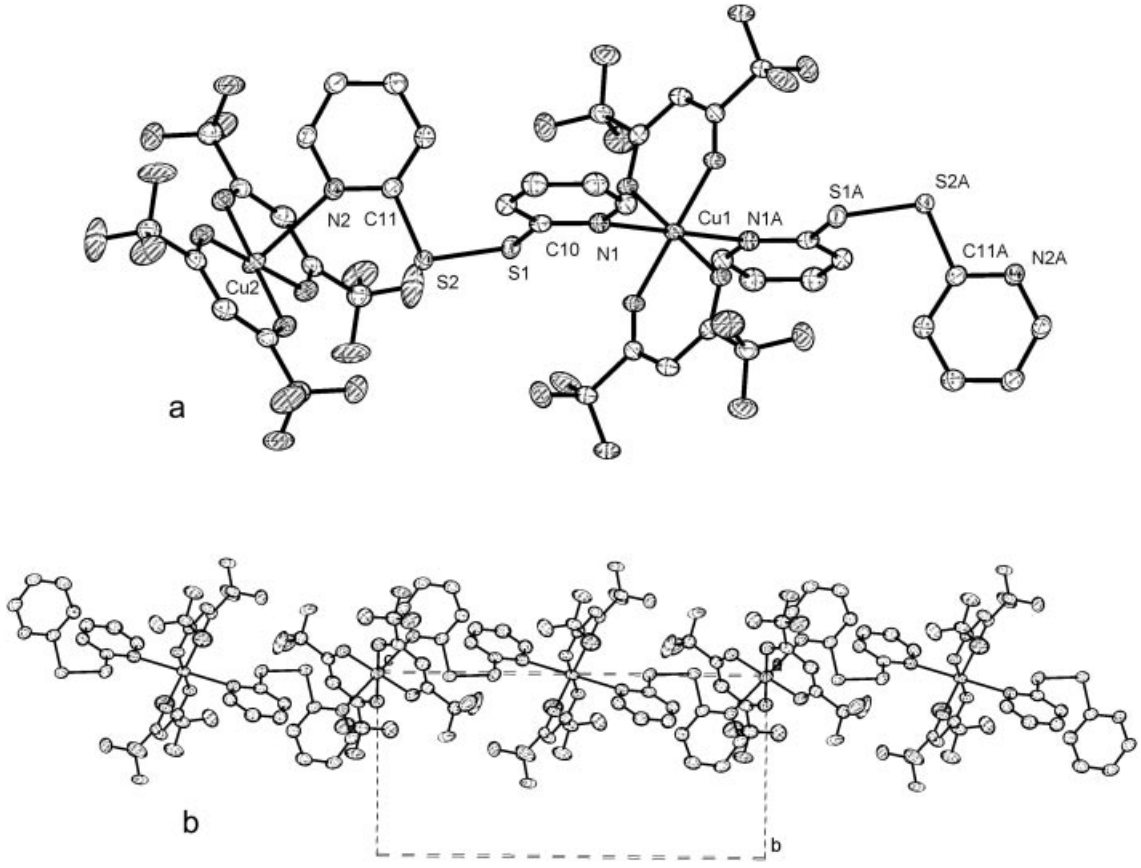

Figure 4. **a**: View of two bonded molecules of **3**, **b**: polymeric chains, shown along the crystallographic *c* axis.

Table 4. Selected bond lengths and angles for compound **3**.

Selected bond lengths [Å]	Selected angles [°]	
Cu(1)–O(1) 1.9572(1)	O(1)–Cu(1)–O(1)#1 180.00(1)	O(2)–Cu(1)–N(1) 88.89(6)
Cu(1)–O(1)#1 1.9572(1)	O(1)–Cu(1)–O(2) 88.10(6)	O(2)#1–Cu(1)–N(1) 91.11(6)
Cu(1)–O(2) 1.9702(1)	O(1)#1–Cu(1)–O(2) 91.90(6)	N(1)#1–Cu(1)–N(1) 180.0
Cu(1)–O(2)#1 1.9702(1)	O(1)–Cu(1)–O(2)#1 91.90(6)	O(4)–Cu(2)–O(4)#2 180.00(1)
Cu(1)–N(1)#1 2.4587(2)	O(1)#1–Cu(1)–O(2)# 188.10(6)	O(4)–Cu(2)–O(3) 92.85(7)
Cu(1)–N(1) 2.4587(2)	O(2)–Cu(1)–O(2)#1 180.00(8)	O(4)#2–Cu(2)–O(3) 87.15(7)
Cu(2)–O(4) 1.9365(1)	O(1)–Cu(1)–N(1)#1 86.79(6)	O(4)–Cu(2)–O(3)#2 87.15(7)
Cu(2)–O(4)#2 1.9365(1)	O(1)#1–Cu(1)–N(1)#1 93.21(6)	O(4)#2–Cu(2)–O(3)#2 92.85(7)
Cu(2)–O(3) 1.9440(2)	O(2)–Cu(1)–N(1)#1 91.11(6)	O(3)–Cu(2)–O(3)#2 180.00(1)
Cu(2)–O(3)#2 1.9440(2)	O(2)#1–Cu(1)–N(1)#1 88.89(6)	O(4)–Cu(2)–N(2) 86.87(6)
Cu(2)–N(2) 2.5968(2)	O(1)–Cu(1)–N(1) 93.21(6)	O(4)#2–Cu(2)–N(2) 93.13(6)
	O(1)#1–Cu(1)–N(1) 86.79(6)	O(3)–Cu(2)–N(2) 90.23(6)
		O(3)#2–Cu(2)–N(2) 89.77(6)

shorter than the **L3** ligand [1.785(2) Å]. Two molecules of **4** are linked through hydrogen bonds between the hydrogen atom of the pyridinium ring and oxygen atoms of the hexafluoroacetylacetonate anion resulting in dimers (Figure 5, b).

[(hfac)Cu($C_{13}H_8N_2S_2OF_3$)] (5)

The molecular structure is shown in Figure 6. Table 1 (compounds **4**–**6**) shows the crystallographic data, while selected bond lengths and angles are summarized in Table 6. The Cu^{II} ion is pentacoordinated to two oxygen atoms of the hfac anion, two nitrogen atoms of two 2-pyridyl sulfide fragments and one carbon atom of the $CC(O)CF_3$ fragment that has been inserted into the S–S bond of the **L3** ligand, giving a new tridentate ligand with two five-membered rings and coordination to the copper atom through nitrogen atoms of the pyridine rings and the terminal carbon atom of the $CC(O)CF_3$ fragment. Although the S–S bond in **L3** is reactive and can undergo several transformations,[13,19b] to the best of our knowledge, this is the first example of rearrangement that involves scission and insertion into the disulfide S–S bond. The environment of the copper atom is of particular interest. The geometry may be described as a highly distorted trigonal bipyramidal with N4, N3, and O4 atoms at the equatorial position and O5 and C29 atoms at

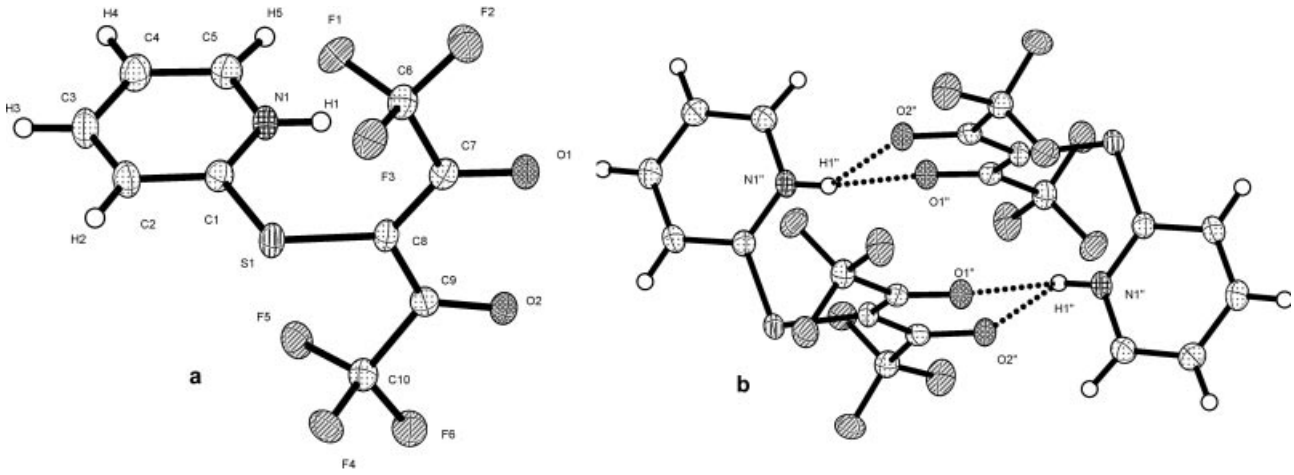

Figure 5. **a**: Molecular structure of **4** (displacement ellipsoids are shown at the 50% probability level), **b**: view of the H bridges between two molecules of this compound.

Table 5. Selected bond lengths and angles for compound **4**.

Selected bond lengths [Å]	Selected angles [°]
S(1)–C(1) 1.7573(1)	C(1)–S(1)–C(8) 104.84(7)
C(7)–O(1) 1.2213(2)	O(1)–C(7)–C(8) 126.40(13)
S(1)–C(8) 1.7601(1)	O(2)–C(9)–C(8) 126.98(13)
C(9)–O(2) 1.2318(2)	
N(1)–H(1) 0.84(2)	

the axial positions. In copper(II) pentacoordinate complexes, trigonal-bipyramidal and square-pyramidal structures are well known; the structures are mostly square pyramidal with various degrees of distortion.[21] Generally, the Cu–L_{axial} bond is longer than the Cu–$L_{equatorial}$ bond in square-pyramidal structures while the opposite is true for the trigonal-bipyramidal geometry. In this compound, all Cu–L distances are similar [2.0034(14) to 2.1461(14) Å]. The Cu–N bond lengths of 2.0074(2) Å and 2.0439(2) Å are very close to the Cu–N bond lengths found in **1** and **2** and are shorter than those in **3**. The ($C_{pyridine\ ring}$–S) and (C_{29}–S) distances are 1.7546(19), 1.7502(19) Å and 1.7915(19), 1.8033(19) Å, respectively, and are similar to those found for **3**, **4**, and **L3**. The (C–Cu) distance is 2.0857(19) Å. The C24–S4–C29 and C19–S3–C29 torsion angles of each of the five-membered rings are similar [102.32(9) and 102.22(9)°], respectively, and these rings are not coplanar [C24–S4–C29–S3 and C19–S3–C29–S4 torsion angles are 102.21(11) and 158.59(10)°, respectively]. Both of the five-membered rings form an angle of 54.94(0.04)°.

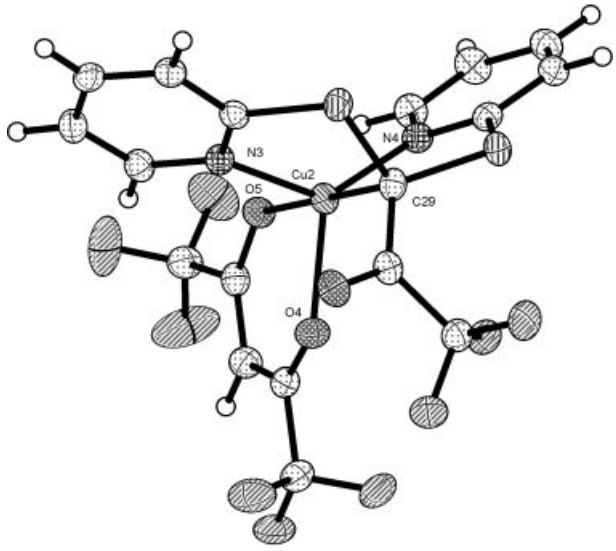

Figure 6. Molecular structure of **5** (displacement ellipsoids are shown at the 50% probability level).

[Cu$_2$(μ-OAc)$_4$(L3)$_2$] (6)

Figure 7 shows the ORTEP drawing of **6**, with the numbering scheme. Table 1 (compounds **4**–**6**) shows the crystal-

Table 6. Selected bond lengths and angles for compound **5**.

Selected bond lengths [Å]	Selected angles [°]	
Cu(1)–O(1) 1.9979(1)	O(1)–Cu(1)–N(1) 90.69(6)	O(5)–Cu(2)–N(4) 91.43(6)
Cu(1)–N(1) 2.0085(2)	O(1)–Cu(1)–N(2) 92.70(6)	O(5)–Cu(2)–N(3) 92.10(6)
Cu(1)–N(2) 2.0226(2)	N(1)–Cu(1)–N(2) 146.57(7)	N(4)–Cu(2)–N(3) 133.57(7)
Cu(1)–C(11) 2.0722(2)	O(1)–Cu(1)–C(11) 176.47(7)	O(5)–Cu(2)–C(29) 179.88(9)
Cu(1)–O(2) 2.2194(1)	N(1)–Cu(1)–C(11) 88.53(7)	N(4)–Cu(2)–C(29) 88.66(7)
Cu(2)–O(5) 2.0033(1)	N(2)–Cu(1)–C(11) 86.07(7)	N(3)–Cu(2)–C(29) 87.89(7)
Cu(2)–N(4) 2.0074(2)	O(1)–Cu(1)–O(2) 85.12(6)	O(5)–Cu(2)–O(4) 85.50(5)
Cu(2)–N(3) 2.0439(2)	N(1)–Cu(1)–O(2) 120.92(6)	N(4)–Cu(2)–O(4) 125.88(6)
Cu(2)–C(29) 2.0857(2)	N(2)–Cu(1)–O(2) 92.51(6)	N(3)–Cu(2)–O(4) 100.55(6)
Cu(2)–O(4) 2.1461(1)	C(11)–Cu(1)–O(2) 98.23(7)	C(29)–Cu(2)–O(4) 94.39(7)

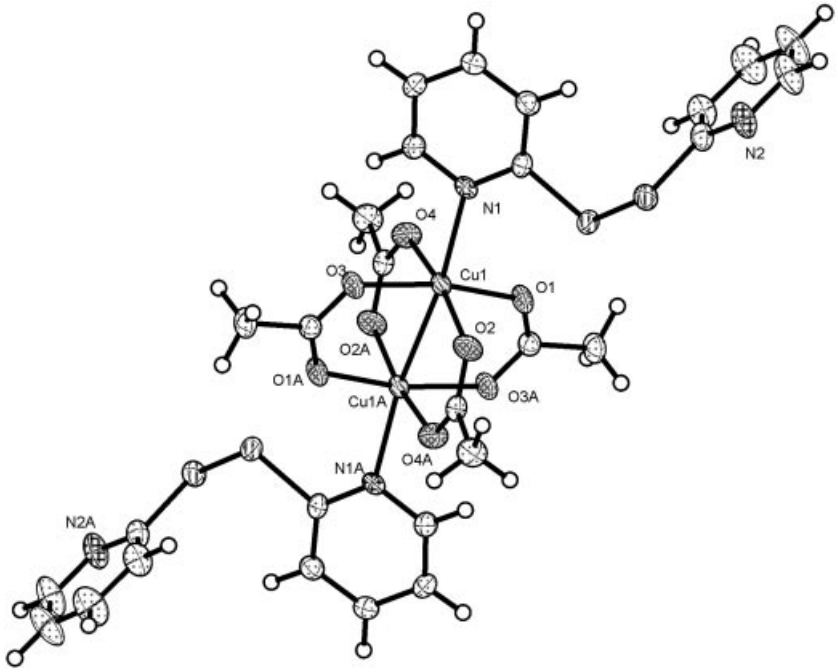

Figure 7. View of two copper centers bonded in compound **6**.

Table 7. Selected bond lengths and angles for compound **6**.

Selected bond lengths [Å]	Selected angles [°]	
Cu(1)–O(1) 1.956(2)	O(1)–Cu(1)–O(2) 90.53(11)	O(2)–Cu(1)–N(1) 102.42(1)
Cu(1)–O(2) 1.965(3)	O(1)–Cu(1)–O(3) 168.72(1)	O(3)–Cu(1)–N(1) 92.16(1)
Cu(1)–O(3) 1.973(2)	O(2)–Cu(1)–O(3) 87.83(1)	O(4)–Cu(1)–N(1) 88.63(1)
Cu(1)–O(4) 1.981(3)	O(1)–Cu(1)–O(4) 89.21(1)	O(1)–Cu(1)–Cu(1)#1 84.28(2)
Cu(1)–N(1) 2.252(3)	O(2)–Cu(1)–O(4) 168.85(1)	O(2)–Cu(1)–Cu(1)#1 85.55(2)
Cu(1)–Cu(1)#1 2.6229(9)	O(3)–Cu(1)–O(4) 90.25(1)	O(3)–Cu(1)–Cu(1)#1 84.47(2)
	O(1)–Cu(1)–N(1) 99.09(1)	O(4)–Cu(1)–Cu(1)#1 83.33(2)

lographic data, and selected bond lengths and angles are summarized in Table 7. The structure consists of the molecular 1:2 adduct $Cu_2(\mu\text{-}OAc)_4(L3)_2$ where the Cu^{II} ion is pentacoordinate to four oxygen atoms of four different acetate anions and one nitrogen atom from the pyridine ring of **L3** to form a square-pyramidal geometry. The Cu(II) center deviates from the mean equatorial plane, defined by four coordinated oxygen atoms, toward the apical nitrogen atom by 0.1536 Å. The Cu–O distances [1.956(2)–1.981(3) Å] are similar to those in its analogous compounds[22] and the Cu–N [2.252(3) Å] distance is shorter than that in **3** but longer than those in **1** and **2** and similar to $[Cu(hfac)_2]_2(pyz)$ [2.25(2) Å].[19a] Four acetate anions bridge two Cu^{II} centers in *syn-syn* fashion to form a $[Cu_2(OAc)_4]$ dinuclear building unit with a Cu–Cu distance of 2.6229(9) Å, which is linked by two **L3** ligands in a *trans* disposition. A similar structure is observed in $[Cu_2(\mu\text{-}OAc)_4(bpt)_2]$bpt [bpt = 1-(2-pyridyl)-2-(2-pyridylsulfanyl)ethane].[23]

Two pyridyl rings within each **L3** ligand are in a *cisoid* arrangement with a C–S–S–C torsion angle of 89.37(17)°, almost similar to that in the free ligand (87.1°). Steric factors produced by the 2,2′-dipyridyl orientation could explain why the molecular compound $[Cu_2(\mu\text{-}OAc)_4(L3)_2]$ (**6**) is formed instead of the polymeric compound $[Cu_2(\mu\text{-}OAc)_4(L3)]_n$. Reactions with dipyridyl ligands with an orientation different from 2,2′ are in progress in order to test how the nature of the ligand affects the structure of the compound.

Magnetic Properties

The magnetic moment of complex **6** at room temperature is 2.05 μ_B. This magnetic moment is smaller than that expected for two magnetically isolated spin $S = 1/2$ centers per molecule. The representation of the magnetic moment versus temperature shows a pronounced decrease until 100 K and drops more slowly to 0.43 μ_B at 2 K. The decrease of the magnetic moment could result from a strong antiferromagnetic coupling. The existence of antiferromagnetic interactions in this complex is also supported by the variation of the magnetic susceptibility with the temperature. Thus, a broad maximum from room temperature to 125 K is observed in the plot of χ_M vs. T. This feature is characteristic of antiferromagnetically coupled Cu^{II} pairs.[24] A paramagnetic tail at very low temperatures is

also observed, which indicates the presence of a paramagnetic impurity. Similar paramagnetic impurities are usually present in complexes with strong antiferromagnetic coupling. Thus, the magnetic data of complex **6** have been analyzed[25] with the isotropic spin Hamiltonian of Equation (1) with $S_1 = S_2 = 1/2$.

$$H = -JS_1S_2 \quad (1)$$

From this spin Hamiltonian the Bleaney–Bowers formula has been derived in which terms corresponding to a paramagnetic impurity (P) and temperature independent paramagnetism (TIP) have been added [Equation (2)]. N, g, β, k, and T have the usual meaning and P is the molar fraction of the noncoupled paramagnetic impurity. In this expression it is assumed that the paramagnetic impurity follows the Curie law and has the same molecular weight and the same g value as complex **6**.

$$\chi_M = \{2Ng^2\beta^2/kT[3 + \exp(-J/kT)] + TIP\}(1 - P) + (Ng^2\beta^2/2kT)P \quad (2)$$

A very good agreement between the experimental and calculated curves of the magnetic moment and the molar susceptibility for complex **6** was observed with this model. The magnetic parameters obtained in the best fit are: g = 2.21, J = –352 cm^{-1}, $TIP = 2.83 \times 10^{-4}$, and P = 2.53%. The agreement factor is 2.95×10^{-5}. Figure 8 shows the experimental and calculated curves for complex **6**.

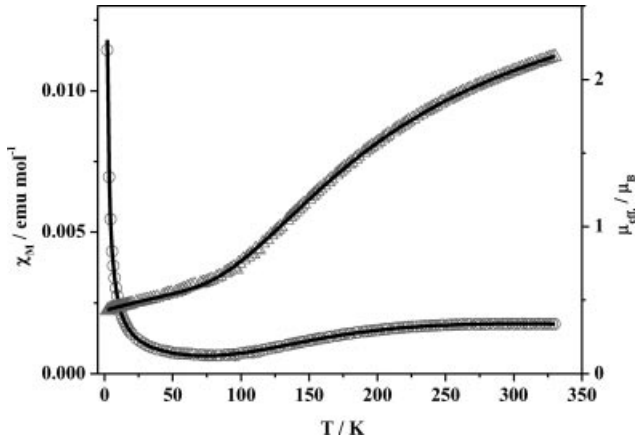

Figure 8. Experimental and calculated curves of χ_M and μ_{eff} vs. T for complex **6**.

The J value indicates that the Cu^{II} centers of each molecule are very strongly antiferromagnetically coupled. This coupling constant is in good agreement with those observed in other tetracarboxylatodicopper(II) complexes.[24–26] Because of the large Cu–Cu distance the antiferromagnetic interaction is probably produced through the carboxylate groups. In fact, it has been pointed out[26d] in similar compounds that the J parameter is more related to the O–Cu–Cu–O bond angles and the O–C–O planes than the Cu–Cu distance.

On the other hand, **1**–**3** shows magnetic moments corresponding to the presence of one unpaired electron per mol of copper at room temperature. The magnetic moment remains almost constant with the temperature and decreases sharply only at very low temperatures. This decrease could be explained by Zeeman level depopulation effects in the applied magnetic field. However, as these complexes form monodimensional systems with very long Cu–Cu distances, mediated by the size of the organic ligands, a weak antiferromagnetic coupling between the Cu^{II} centers could also be possible. Thus, to fit these magnetic data we have considered the molecular field approximation applied to a paramagnetic model with S = 1/2 [Equation (3)]. $\chi_{Cu} = Ng^2\beta^2/4kT$, z is the number of neighbors and J is the magnitude of the interaction of the Cu^{II} centers.

$$\chi_M = \frac{\chi_{Cu}}{1 - [2\,zJ/N\,g^2\,\beta^2]\chi_{Cu}} \quad (3)$$

The parameters of the best fits are collected in Table 8. Figure 9 shows the experimental and calculated curves for complex **2**. Similar curves have been obtained for the other complexes. The zJ values (from –0.45 to –0.16 cm^{-1}) are very low, in accordance with the presence of a very weak antiferromagnetic interaction between the copper(II) centers.

Table 8. Magnetic parameters for complexes **1**–**3** obtained from the fits of the magnetic moment as a function of temperature.

Compound	g	J [cm^{-1}]	σ^{2}[a]
1	2.20	–0.45	4.33×10^{-5}
2	2.20	–0.24	7.55×10^{-5}
3	2.17	–0.16	9.39×10^{-5}

[a] $\sigma^2 = \Sigma(\mu_{eff.\ calcd.} - \mu_{eff.\ exp.})^2 / \Sigma\mu_{eff.\ exp.}{}^2$, [$\sigma^2 = \Sigma(\chi_{mol\ calcd.} - \chi_{mol\ exp.})^2 / \Sigma\chi_{mol\ exp.}{}^2$].

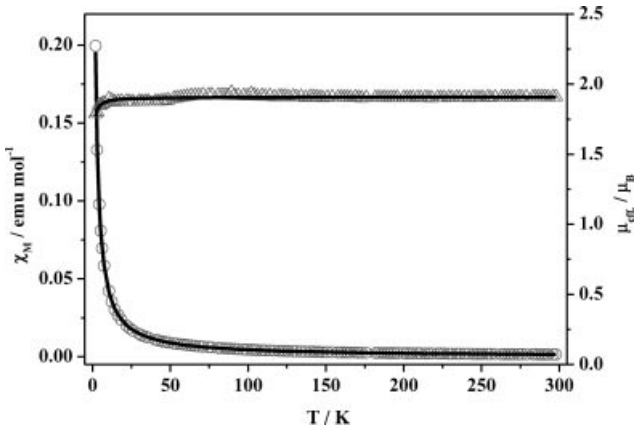

Figure 9. Experimental and calculated curves of χ_M and μ_{eff} vs. T for complex **1**.

Thermal Properties

The thermal properties of the compounds were examined by thermal gravimetric analysis (TGA/DTA) and differential scanning calorimetry (DSC). Compounds **1**–**3** and **6** were heated to 600 °C under a nitrogen atmosphere. TGA data suggest that the framework of **1** is stable up to 170° and show a weight loss of 60.80% (calcd. 60.30%) from 170 to 325 °C corresponding to the loss of one 1,2-di(2-pyridyl) butadiyne (**L1**) and one hfac chelating ligand per formula unit. Further weight loss is observed above 325 °C, with CuO remaining as a black powder (observed 11.82%, calcd. 11.67%). Compound **2** is also stable up to 170 °C, and in the temperature range 170–435 °C it undergoes two weight loss steps corresponding to one 1,2-bis(2-pyridylethynyl)-thiophene ligand (**L2**) and one hfac chelating ligand (found 64.42%, calcd. 64.57%). Above 435 °C, weight loss is also observed and the black powdery product once again is CuO (found 10.62%, calcd. 10.40%). Compound **3** is stable up to 80 °C, and up to 415 °C undergoes three weight loss steps; the first two (up to 160 °C and up to 215 °C) produce a loss of 15.60% and 15.45%, respectively, each corresponding to a 2-pyridyl sulfide fragment (calcd. 15.77%). In the range 215–415 °C, the loss of one hfac anion is observed (found 29.50, calcd. 29.67%). Above 415 °C, the weight loss observed is assigned to CuO (obsd. 11.20%, calcd. 11.39%). Compound **6** is stable up to 125 °C; in the 125–260 °C and 260–400 °C ranges, a loss of two 2,2′-dipyridyl disulfide (**L3**) ligands and three acetate anions, respectively, is observed. Above 400 °C, weight loss is also observed (10.35%) and is attributed to CuO (calcd. 10.52%).

This behavior is common for organic–inorganic coordination polymers consisting of $Cu(hfac)_2$ cations and *N*,*N*′-bidentate-type ligands.[13] DSC analyses of hermetically sealed samples of **1** and **2** display sharp endothermic peaks at 126.4 °C and 177.2 °C, respectively, which correspond to the melting point.

Conclusions

Six new compounds generated from the reactions of 1,2-di(2-pyridyl)-1,3-butadiyne (**L1**), 2,5-bis(2-pyridylethynyl)-thiophene (**L2**), and 2,2′-dipyridyl disulfide (**L3**) with $Cu(hfac)_2$ and copper acetate have been synthesized and structurally characterized by X-ray diffraction.

The **1**–**3** coordination polymers described in this paper are some of the first reported examples of polymers based on dipyridyl ligands in 2,2′-positions and illustrate that the positional orientation of pyridyl nitrogen atoms and the nature of the ligands (**L1** and **L2** are rigid, **L3** is flexible) affects the structure during the self-assembly process. Moreover, new interesting transformations take place from 2,2′-dipyridyl disulfide (**L3**), because of the reactivity of the S–S bond, and the organic and mononuclear copper compounds **4** and **5** are obtained. In **5**, as a result of rearrangement, a copper–carbon bond is formed. The reaction of **L3** with copper acetate does not lead to polymeric compounds but a molecular complex **6** (1:2 adduct). Further studies of these ligands with transition metal salts are in progress in our laboratories.

Experimental Section

General: All the solvents were of reagent grade quality and were used as received. 2,5-Dibromothiophene (Aldrich), 2-ethynylpyridine (Aldrich), tetramethylethylenediamine (Aldrich), $PdCl_2$ (Aldrich), CuI (Aldrich), $Cu(hfac)_2{\cdot}H_2O$ (hfac = hexafluoroacetylacetonate) (Aldrich), and 2,2′-dipyridyl disulfide (**L3**) (Lancaster) were used as received. Et_3N (Fluka) was distilled from KOH immediately before use. $Pd(PPh_3)_4$[27] and the **L1** ligand[28] were prepared according to a literature procedure and **L2** was synthesized by us from a literature method.[29] The ^1H and ^{13}C NMR spectra were recorded with Bruker AMX-300 or 500 instruments. Solid-state NMR measurements were performed at room temperature with a Bruker AV 400WB (9.4 T) with a 4 mm MAS probehead. Infrared spectra were measured with a Perkin–Elmer 1650 infrared spectrometer. Elemental analyses were performed by the Microanalytical Laboratory of the University Autónoma of Madrid with a Perkin–Elemer 240 B microanalyzer. The Mass spectrum was measured with a VG-Autospec mass spectrometer for FAB by the Mass Laboratory of the University Autónoma of Madrid. Single-crystal diffraction experiments were performed with samples mounted on a glass fiber and transferred to a Bruker SMART 6 K CCD area-detector three-circle diffractometer with a Rigaku Rotating Anode (Cu-K_α radiation, λ = 1.54178 Å) generator equipped with Goebel mirrors at settings of 50 kV and 100 mA. X-ray data were collected at 100 K, with a combination of six runs at different φ and 2θ angles, 3600 frames. The data were collected using 0.3° wide ω scans with a crystal-to-detector distance of 4.0 cm.

The substantial redundancy in data allows empirical absorption corrections (SADABS) to be applied using multiple measurements of symmetry-equivalent reflections.

The raw intensity data frames were integrated with the SAINT program, which also applied corrections for Lorentz and polarization effects.

The software package SHELXTL version 6.10 was used for space group determination, structure solution, and refinement. The space group determination was based on a check of the Laue symmetry and systematic absences and was confirmed using the structure solution. The structures were solved by direct methods (SHELXS-97), completed with difference Fourier syntheses, and refined with full-matrix least-squares using SHELXL-97 minimizing $\omega(F_o^2 - F_c^2)^2$. Weighted *R* factors (R_w) and all goodness of fits *S* are based on F^2; conventional *R* factors (*R*) are based on *F*. All scattering factors and anomalous dispersion factors are contained in the SHELXTL 6.10 program library. Table 1 contains crystal data for complexes **1**–**6**.

CCDC-264487, -264488, -287409, -287410, -287412, and -287878 contain the supplementary crystallographic data for complexes **1**–**6**. These data can be obtained free of charge from The Cambridge Crystallographic Data Centre via www.ccdc.cam.ac.uk/data_request/cif. The variable-temperature magnetic susceptibilities were measured on polycrystalline samples with a Quantum Design MPMSXL SQUID (Superconducting Quantum Interference Device) susceptometer over a temperature range of 2 to 300 K (Complutense University of Madrid). All data were corrected for the diamagnetic contribution of both the sample holder and the compound to the susceptibility. The molar diamagnetic corrections for the complexes were calculated based on Pascal's constants.

The thermal properties were examined by thermal gravimetric analysis (TGA) and differential scanning calorimetry (DSC). The gravimetric data were obtained on a Seiko DTA/TG 320 U using an open pan, which was purged with N_2 and at a heating rate of 5 °C/min. The calorimetric data were obtained with a Perkin–Elmer Pyris 1DSC instrument using a sealed pan with a heating rate of 5 °C/min. The melting points were also obtained by using a conventional melting point apparatus.

Synthesis of 1,2-Bis(2-pyridylethynyl)thiophene (L2): A mixture of 2,5-dibromothiophene (1.75 g, 7.27 mmol), 2-ethynylpyridine (3.00 g, 29 mmol), $Pd(PPh_3)_4$ (1.26 g, 1.09 mmol), and CuI (0.192 g, 1.0 mmol) in triethylamine (40 mL) and THF (40 mL) was stirred under Ar at 70 °C for 20 h. The solution was cooled to room temperature and after evaporation of the solvent a brown solid was obtained. The crude product was extracted with several portions of ether, filtered and evaporated at reduced pressure. The residue was purified by chromatography on silica gel eluting with ether/CH_2Cl_2 (1:1). The product 1,2-bis(2-pyridylethynyl)thiophene (**L2**) was isolated as a yellow solid (1.78 g, 85%); m.p. 115–116 °C. (KBr): $\tilde{\nu}$ = 2204 (s, $\nu_{C\equiv C}$), 1576 and 1556 (s, $\nu_{C=C,}$ $\nu_{C=N}$, conj), 987 (vs, py), 774 (m) and 737 (s, py-H) cm^{-1}. ^1H NMR ([D$_6$]acetone, 300 MHz): δ = 8.63 (d, J = 4.3 Hz, 2 H), 7.85 (td, J = 2.7and 0.67 Hz, 2 H), 7.64 (dt, J = 2.7 and 0.3 Hz, 2 H), 7.45 (s, 2 H), 7.40 (td, J = 2.0 and 0.3 Hz, 2 H) ppm. ^{13}C NMR (500 MHz, $CDCl_3$): δ = 81.9 (C8), 93.1 (C7), 123.1(C3), 124.6 (C5), 127.1 (C9), 136.2 (C4), 133.2 (C10), 142.8 (C2), 150.2 (C6) ppm. MS (FAB$^+$): m/z (%) = 286 [M$^+$]. $C_{18}H_{10}N_2S$ (287): calcd. C 75.52, H 3.49, N 9.79; found C 75.58, H 3.43, N 9.70.

Synthesis of $[Cu(hfac)_2L1]_n$ (1): A solution of $Cu(hfac)_2{\cdot}H_2O$ (110 mg; 0.245 mmol) in CH_2Cl_2 (5 mL) was slowly layered onto a solution of **L$_1$** (50 mg; 0.245 mmol) in CH_2Cl_2 (5 mL). The solution was allowed to stand at 0 °C for 2 d. Green crystals were obtained (150.3 mg, 90%). M.p. 133 °C. IR (KBr): $\tilde{\nu}$ = 3077 (w), 1654 (s), 1592 (m), 1574 (s), 1561 (s), 1525 (s), 1475 (s), 1459 (vs), 1425 (s), 1258 (vs), 1240 (m), 1197 (vs), 1146 (vs), 798 (m), 774 (vs), 733 (s), 666 (s), 629 (m), 583 (m), 532 (s) cm^{-1}. $C_{24}H_{10}CuF_{12}N_2O_4$ (681.88): calcd. C 42.47, H 1.48, N 4.11; found C 42.24, H 1.50, N 4.08.

Synthesis of $[Cu(hfac)_2L2]_n$ (2): A solution of **L2** (40 mg, 0.139 mmol) in CH_2Cl_2 (2 mL) was slowly added to a CH_2Cl_2 solution (2 mL) of $Cu(hfac)_2{\cdot}H_2O$ (66.8 mg, 0.139 mmol). The solution was allowed to stand at room temperature. After 2 d a yellowish solution appeared. The solvent was then slowly evaporated over a period of 1 d to half the initial volume. The solution was allowed to stand at 0 °C for 2 d and yellow crystals were obtained (90.26 mg, 85%). M.p. 175 °C. IR (KBr): $\tilde{\nu}$ = 3100 (w), 2209 (vs), 1644 (vs), 1594 (vs), 1561 (vs), 1546 (vs), 1523 (vs), 1471 (vs), 1433 (s), 1337 (m), 1320 (m), 1250 (vs), 1196 (vs), 1132 (vs), 1084 (vs), 808 (vs), 790 (vs), 771 (vs), 756 (s), 740 (s), 667 (vs), 583 (vs), 521 (s) cm^{-1}. $C_{28}H_{12}CuF_{12}N_2O_4S$ (764): calcd. C 44.00, H 1.57, N 3.67; found C 43.98, H 1.54, N 3. 63.

Synthesis of $[Cu(hfac)_2L3]_n$ (3), Zwitterionic Compound 4 and $[(hfac)Cu(C_{13}H_8N_2S_2OF_3)]$ (5). Method (a): A solution of **L3** (100 mg, 0.455 mmol) in CH_2Cl_2 (3 mL) was added to a CH_2Cl_2 solution (8 mL) of $Cu(hfac)_2{\cdot}H_2O$ (217 mg, 0.455 mmol). After the mixture was left for 2 d at room temperature, the solvent was evaporated. After recrystallization in CH_2Cl_2/hexane (1:1), **3** was obtained as a green solid (206.2 mg, 65%), **4** as a yellow solid (36.08 mg, 25%), and **5** as a violet solid (13.65 mg, 5%). X-ray quality crystals of **3** and **4** were grown by slow evaporation of CH_2Cl_2 solutions at –10 °C and room temperature, respectively. Crystals suitable for X-ray analysis of **5** were obtained by slow evaporation of hexane solutions at room temperature.

3: M.p. 88 °C. IR (KBr): $\tilde{\nu}$ = 3055 (w), 1641 (vs), 1611 (w), 1580 (s), 1561 (s), 1535 (m), 1485 (vs), 1472 (vs), 1455 (vs), 1420 (vs), 1255 (vs), 1224 (vs), 1210 (vs), 1147 (vs), 807 (s), 799 (s), 760 (s), 679 (s), 596 (s), 527 (m) cm^{-1}. $C_{20}H_{10}CuF_{12}N_2O_4S_2$ (697.96): calcd. C 34.41, H 1.43, N 4.01, S 9.17; found C 34.32, H 1.48, N 3.97, S 9.23.

4: M.p. 102 °C. IR (KBr): 3103 (w), 3070 (w), 1679 (vs), 1606 (m), 1583 (s), 1507 (m), 1452 (s), 1420 (s), 1260 (m), 1203 (vs), 1203 (vs), 837 (m), 803 (m), 758 (s), 722 (s), 520 (m) cm^{-1}. ^1H NMR ($CDCl_3$, 300 MHz): δ = 8.40 (d, J = 4.3 Hz, 1 H), 7.56 (dd, J = 3.7 and 1.0 Hz, 1 H), 7.33 (dd, J = 2.3 and 1.8 Hz, 1 H) ppm. ^1H NMR (CD_2Cl_2, 300 MHz): δ = 8.68 (d, J = 4.2 Hz, 1 H),8.20 (t, J = 2.6 Hz, 1 H), 7.74 (d, J = 1.05 Hz, 1 H), 7.62 (t, J = 2.24 Hz, 1 H) ppm. $C_{10}H_5NO_2SF_6$ (317.21): C 37.82, H 1.58, N 4.42, S 10.10; found C 3.72, H 1.61, N 4.37, S 9.99.

5: M.p. 150 °C. IR (KBr): $\tilde{\nu}$ = 3076 (w), 1673 (vs), 1650 (vs), 1611 (w), 1593 (s), 1559 (s), 1522 (m), 1486 (vs), 1457 (vs), 1421 (vs), 1302 (s), 1285 (s), 1260 (vs), 1203 (vs), 1205 (vs), 1147 (vs), 1051 (s), 1013 (s), 879 (m), 807 (m), 797 (m), 789 (s), 770 (vs), 760 (vs), 729 (s), 703 (s), 679 (s), 668 (s), 586 (m), 527 (m), 486 (m), 410 (m) cm^{-1}. ^1H NMR ($CDCl_3$, 300 MHz): 8.00 (br. s, 2 H), 7.63 (br. s, 2 H) ppm. $C_{18}H_9CuO_3N_2S_2F_9$ (599.93): calcd. C 36.00, H 1.50, N 4.07, S 10.67; found C 36.18, H 1.47, N 4.06, S 10.58.

Method (b): A solution of **L3** (100 mg, 0.455 mmol) in MeOH (2 mL) was added to a solution of $Cu(hfac)_2{\cdot}H_2O$ (217 mg, 0.455 mmol, 6 mL) in the same solvent. After the solution was slowly evaporated at room temperature for 2 d, only green crystals of **3** were obtained (285.8 mg, 90%).

Method (c): $Cu(hfac)_2{\cdot}H_2O$ (434 mg, 0.91 mmol) in CH_2Cl_2 (15 mL) was added to a solution of **L3** (200 mg, 0.91 mmol) in CH_2Cl_2 (6 mL). The reaction was monitored by FT-IR spectroscopy. After the mixture was refluxed for 48 h, the pH was checked and an acidic pH was observed. The solvent was removed under vacuum and the residue was extracted with hexane giving a violet solution. Slow evaporation of the solvent gave crystals of **5** (49.13 mg, 18%) suitable for X-ray analysis. The insoluble residue in hexane was redissolved in CH_2Cl_2 and stood for about 3 d at –10 °C. Yellow crystals of **4** were obtained (101.0 mg, 70%). Similar results were obtained when the reaction was carried out in MeOH.

Synthesis of $[Cu_2(\mu\text{-}OAc)_4(L3)_2]$ (6): A solution of $Cu(OAc)_2{\cdot}H_2O$ (55 mg, 0.28 mmol) in CH_3OH (15 mL) was added to a solution of **L3** (62 mg, 0.28 mmol) in CH_3OH (3 mL). The solution was left for 2 d at room temperature and for about 2 d in the refrigerator (–10 °C). Blue crystals of copper acetate were isolated by filtration; the solution was filtered off, the solvent was removed under vacuum and the residue was washed several times with hexane/CH_2Cl_2 (10:2) to isolate **L3**. Extraction of the solid with CH_2Cl_2/CH_3OH (1:1), followed by slow solvent evaporation afforded green crystals of **6** (87 mg, 50%). M.p. 205 °C. IR (KBr): $\tilde{\nu}$ = 3055 (w), 1618 (vs), 1573 (vs), 1561 (vs), 1457 (vs), 1427 (vs), 1418 (vs), 1347 (m), 1288 (m), 1163 (s), 1117 (s), 1051 (s), 1000 (s), 774 (vs), 754 (vs), 719 (s), 682 (vs), 627 (vs) cm^{-1}. $C_{28}H_{28}Cu_2N_4O_8S_4$ (803.86): calcd. C 41.84, H 3.49, N 6.97, S 15.94; found C 41.40, H 3.48, N 7.08, S 15.66.

Acknowledgments

We express great appreciation to the Dirección General de Investigación Científica y Tecnológica (Grant n°. BQU 2002-02522, MAT 2004-22102-E Spain). We are grateful to the student J. Toledano for the help in the preparation of the compounds **L2** and **2**

and to Dra. R. Rojas (Instituto de Materiales, CSIC, Spain) for the DSC and DTA/TG measurements.

[1] a) S. Kitagawa, S. Noro, *Comprehensive Coord. Chem. II* (Eds.: J. A. McCleverty, T. J. Meyer) Elsevier, Oxford, **2004**, vol. 7, p. 231; b) L. Brammer, *Chem. Soc. Rev.* **2004**, *33*, 476; c) T. Yuen, C. L. Lin, T. W. Mihalisin, M. A. Lawandy, J. Li, *J. Appl. Phys.* **2000**, *87*, 6001; d) J. L. Manson, A. M. Arif, C. D. Incarvito, L. M. Liable-Sands, A. L. Reinghold, J. S. Miller, *J. Solid State Chem.* **1999**,*145*, 369; e) F. Lloret, G. De Munno, M. Julve, J. Cano, R. Ruiz, A. Caneschi, *Angew. Chem. Int. Ed. Engl.* **1998**, *37*, 135.

[2] a) M. E. Kosal, J.-H. Chou, S. R. Wilson, K. S. Suslick, *Nat. Mater.* **2002**, *1*, 118; b) S. Kitagawa, R. Kitaura, S. Noro, *Angew. Chem. Int. Ed.* **2004**, *43*, 2334; c) M. Kondo, T. Okubo, A. Asami, S. Noro, T. Yoshimoti, S. Kitagawa, T. Ishii, H. Matzusaka, K. Seki, *Angew. Chem. Int. Ed.* **1999**, *38*, 140.

[3] a) H. Hou, X. Meng, Y. Song, Y. Fan, Y. Zhu, H. Lu, C. Du, W. Shao, *Inorg. Chem.* **2002**,*41*, 4068; b) W. Lin, Z. Wang, L. Ma, *J. Am. Chem. Soc.* **1999**, *121*, 11249; c) C. Chen, K. S. Suslick, *Coord. Chem. Rev.* **1993**, *128*, 293.

[4] a) M. Albrecht, M. Lutz, A. L. Spek, G. van Koten, *Nature* **2000**, *406*, 970; b) L. G. Beauvais, M. P. Sores, J. R. Long, *J. Am. Chem. Soc.* **2000**, *122*, 2763.

[5] a) M. Munakata, L. P. Wu, T. Kuroda-Sowa, *Adv. Inorg. Chem.* **1999**, *46*, 173; b) A. J. Blake, N.-R. Champness, P. Hubberstey, W. S. Li, M. A. Withersby, M. Schroder, *Coord. Chem. Rev.* **1999**, *183*, 117; c) O. M. Yaghi, H. Li, C. Davis, D. Richardson, T. L. Groy, *Acc. Chem. Res.* **1998**, *31*, 474; d) O. S. Jung, Y. J. Kim, Y. A. Lee, J. K. Park, H. K. Chae, *J. Am. Chem. Soc.* **2000**, *122*, 9921.

[6] a) N. G. Pschirer, D. M. Ciurtin, M. D. Smith, U. H. F. Bunz, H. C. zur Loye, *Angew. Chem. Int. Ed.* **2002**, *41*, 603; b) K. Biradha, Y. Hongo, M. Fujita, *Angew. Chem. Int. Ed.* **2000**, *39*, 3843; c) D. Hargman, R. P. Hammond, R. Haushalter, J. Zubieta, *Chem. Mater.* **1998**, *10*, 2091; d) M. Fujita, Y. J. Kwon, S. Washizu, K. Ogura, *J. Am. Chem. Soc.* **1994**, *116*, 1151.

[7] Z. Huang, H.-B. Song, M. Du, S.-T. Chen, X.-H. Bu, *Inorg. Chem.* **2004**, *43*, 931.

[8] a) A. Jain, T. T. Kodas, T. S. Corbitt, J. M. Hampden-Smith, *Chem. Mater.* **1996**, *8*, 1119; b) R. J. Puddephatt, *Polyhedron* **1994**, *13*, 1233; c) J. Pinkas, J. C. Huffman, D. V. Baxter, M. H. Chisholm, K. G. Caulton, *Chem. Mater.* **1995**, *7*, 1589.

[9] W. Fujita, K. Awaga, *J. Am. Chem. Soc.* **2001**, *123*, 3610.

[10] a) Y. Sano, M. Tanaka, N. Koga, M. Matsuda, H. Iwamura, P. Rabu, M. Drillon, *J. Am. Chem. Soc.* **1997**, *119*, 8246; b) S. Karasawa, Y. Sano, T. Akita, N. Koga, T. Itoh, H. Iwamura, P. Rabu, M. Drillon, *J. Am. Chem. Soc.* **1998**, *120*, 10080; c) Y. Ishimaru, M. Kitano, H. Kumada, N. Koga, H. Iwamura, *Inorg. Chem.* **1998**, *37*, 2273; d) A. Kamiyama, T. Noguchi, T. Kajiwara, T. Ito, *Inorg. Chem.* **2002**, *41*, 507.

[11] M. B. Zaman, M. D. Smith, D. M. Ciurtin, H. C. zur Loye, *Inorg. Chem.* **2002**, *41*, 4895.

[12] a) L. S. Higashi, M. Lundeen, K. Seff, *J. Am. Chem. Soc.* **1978**, *100*, 8101; b) L. S. Higashi, M. Lundeen, E. Hilti, K. Seff, *Inorg. Chem.* **1977**, *16*, 310.

[13] Y. B. Dong, M. D. Smith, R. C. Layland, H. C. zur Loye, *Inorg. Chem.* **1999**, *38*, 5027.

[14] M. B. Zaman, K. A. Udachin, J. A. Ripmeester, *Cryst. Eng. Commun.* **2002**, *4*, 613.

[15] R. Horikoshi, T. Mochida, H. Moriyama, *Inorg. Chem.* **2001**, *40*, 2430.

[16] A. Escuer, T. Comas, J. Ribas, R. Vincent, X. Xolans, C. Zanchini, D. Gatteschi, *Inorg. Chim. Acta* **1989**, *162*, 97.

[17] a) J. L. Manson, *Inorg. Chem.* **2003**, *42*, 2602; b) S. Karasawa, H. Kumada, N. Koga, H. Iwamura, *J. Am. Chem. Soc.* **2001**, *123*, 1387; c) M. J. Plater, M. R. Foreman, A. M. Z. Slawin, *Inorg. Chim. Acta* **2000**, *303*, 132.

[18] a) J. Luo, M. Hong, R. Wang, D. Yuan, R. Cao, L. Han, Y. Xu, Z. Lin, *Eur. J. Inorg. Chem.* **2003**, 3623; b) I. Kinoshita, L. J. Wrigth, S. Kubo, K. Kimura, A. Sakata, T. Yana, R. Miyamoto, T. Nishioka, K. Isobe, *Dalton Trans.* **2003**, 1993.

[19] a) R. C. E. Belford, D. E. Fenton, M. R. Truter, *J. Chem. Soc., Dalton Trans.* **1974**, 17; b) R. C. E. Belford, D. E. Fenton, M. R. Truter, *J. Chem. Soc., Dalton Trans.* **1972**, 2208.

[20] N. V. Raghavan, K. Seff, *Acta Crystallogr., Sect. B* **1977**, *33*, 38.

[21] M. Melnik, M. Kabesova, M. Dunaj-Jurco, C. E. Holloway, *J. Coord. Chem.* **1997**, *41*, 35.

[22] a) M. Du, Z. Huang, S.-t. Chen, Y.-M. Guo, *Inorg. Chem.* **2003**, *42*, 552; b) Z. Huang, H.-B. Song, M. Du, S.-T. Chen, X.-H. Bu, *Inorg. Chem.* **2004**, *43*, 931.

[23] S. C. Davies, M. C. Durrant, D. L. Hughes, K. Leidenberger, C. Stapper, R. L. Richards, *J. Chem. Soc., Dalton Trans.* **1997**, 2409.

[24] J. Mrozinski, *Coord. Chem. Rev.* **2005**, *249*, 2534.

[25] O. Kahn, *Molecular Magnetism*, VCH Publishers, Inc., USA, **1993**, p. 107.

[26] For example, see: a) Z. Huang, H.-B. Song, M. Du, S.-T. Chen, X.-H. Bu, J. Ribas, *Inorg. Chem.* **2004**, *43*, 931; b) P. Stachová, D. Valigura, M. Koman, M. Melník, M. Korabik, J. Mrozinski, T. Glowiak, *Polyhedron* **2004**, *23*, 1303; c) M. Du, X.-H. Bu, Z. Huang, S.-T. Chen, Y.-M. Guo, C. Díaz, J. Ribas, *Inorg. Chem.* **2003**, *42*, 552; d) M. Rusjan, Z. Chaia, O. E. Piro, D. Guillond, F. D. Cukiernik, *Acta Crystallogr., Sect. B* **2000**, *56*, 666.

[27] D. R. Coulson, *Inorg. Synth.* **1990**, *28*, 107.

[28] J. G. Rodríguez, R. Martínez-Villamil, F. H. Cano, I. Fonseca, *J. Chem. Soc., Perkin Trans. 1* **1997**, 709.

[29] K. Sonogashira, Y. Tohda, N. Hagihara, *Tetrahedron Lett.* **1975**, *16*, 4467.

Received: October 28, 2005
Published Online: May 12. 2006

